AIP | Review of Scientific Instruments

Design and implementation of a novel portable atomic layer deposition/chemical vapor deposition hybrid reactor

Sathees Kannan Selvaraj, Gregory Jursich, and Christos G. Takoudis

Citation: Review of Scientific Instruments **84**, 095109 (2013); doi: 10.1063/1.4821081
View online: http://dx.doi.org/10.1063/1.4821081
View Table of Contents: http://scitation.aip.org/content/aip/journal/rsi/84/9?ver=pdfcov
Published by the AIP Publishing

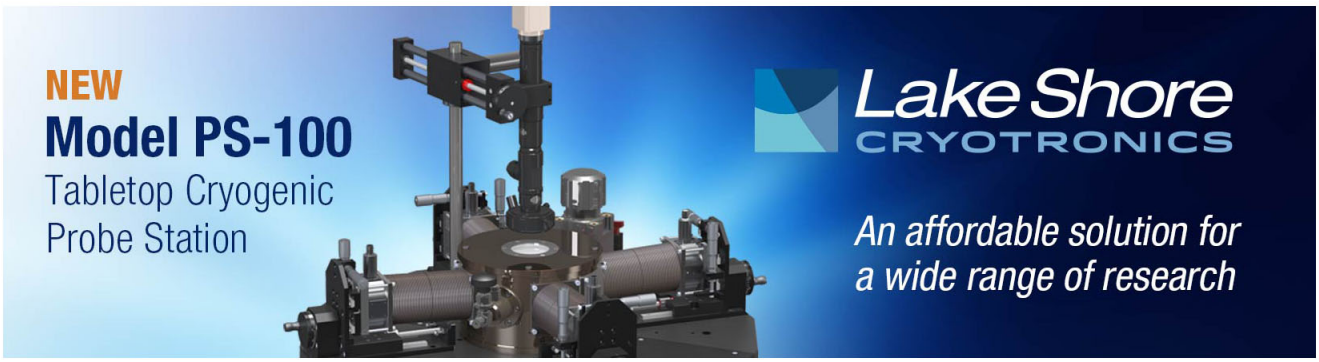

Design and implementation of a novel portable atomic layer deposition/chemical vapor deposition hybrid reactor

Sathees Kannan Selvaraj,[1] Gregory Jursich,[2] and Christos G. Takoudis[1,2,a)]
[1]*Department of Chemical Engineering, University of Illinois at Chicago, Chicago, Illinois 60607, USA*
[2]*Department of Bioengineering, University of Illinois at Chicago, Chicago, Illinois 60607, USA*

(Received 29 May 2013; accepted 26 August 2013; published online 16 September 2013)

We report the development of a novel portable atomic layer deposition chemical vapor deposition (ALD/CVD) hybrid reactor setup. Unique feature of this reactor is the use of ALD/CVD mode in a single portable deposition system to fabricate multi-layer thin films over a broad range from "bulk-like" multi-micrometer to nanometer atomic dimensions. The precursor delivery system and control-architecture are designed so that continuous reactant flows for CVD and cyclic pulsating flows for ALD mode are facilitated. A custom-written LabVIEW program controls the valve sequencing to allow synthesis of different kinds of film structures under either ALD or CVD mode or both. The entire reactor setup weighs less than 40 lb and has a relatively small footprint of 8 × 9 in., making it compact and easy for transportation. The reactor is tested in the ALD mode with titanium oxide (TiO_2) ALD using tetrakis(diethylamino)titanium and water vapor. The resulting growth rate of 0.04 nm/cycle and purity of the films are in good agreement with literature values. The ALD/CVD hybrid mode is demonstrated with ALD of TiO_2 and CVD of tin oxide (SnO_x). Transmission electron microscopy images of the resulting films confirm the formation of successive distinct TiO_2-ALD and SnO_x-CVD layers. © *2013 AIP Publishing LLC*. [http://dx.doi.org/10.1063/1.4821081]

I. INTRODUCTION

Functional thin films form the backbone of many technologies in microelectronics, optoelectronics, and chemical industries by providing functional thin film surface coatings related to catalysis, solar panels, and batteries,[1–6] for example. These films function in diverse thickness scale from micrometers to nano-meters. Often, functionality of such films requires high purity at precise composition. Even minuscule impurity incorporation can be detrimental on device performance; therefore, it becomes necessary to avoid impurity contamination. Multi-chamber cluster tools are commonly employed to avoid contamination during processing steps.[7] Though they have the advantage of using a separate chamber for each processing step, they are rather complex by design and expensive. One simple approach to avoid contamination due to ambient exposure is performing all deposition processing within a single chamber without breaking vacuum and potentially exposing film materials internal to the device to ambient environment. For multilayer film structures, this is best accomplished by integrating different film deposition techniques within a single chamber.[8–14]

A wide variety of deposition methods are used for different thin film applications. Atomic layer deposition (ALD) and chemical vapor deposition (CVD) methods are efficient methods for conformal films which are complementary to each other with advantages and limitations. ALD, for example, has precise thickness and composition control along with superior conformality,[15] whereas growth rate of ALD is typically an order of magnitude or two lower than that of other deposition techniques such as CVD or physical vapor deposition (PVD).[16,17] Combining ALD and CVD in one reactor system enables faster film growth for thicker films along with precisely controlled thickness and composition for thinner films when performed by ALD. For example, ALD can be used to deposit ultra thin adhesion layers for a copper interconnect application followed by a thicker copper layer[13] by CVD for the Cu interconnect all without vacuum break in a single deposition chamber. This will ensure a pristine ALD/CVD interface, free from contaminants of the ambient environment. There are few reports on hybrid thin film deposition systems in the open literature. For example, Martin *et al.*[10] combined reactive magnetron sputtering and e-beam evaporation; Kala *et al.*[12] coupled nano-particle synthesis setup with thin film evaporation deposition setup to form nano-particle incorporated thin film structures. Zeng *et al.*[8] combined PVD and CVD to deposit superconducting MgB_2 thin films. Reid and Dip[9] used CVD and ALD in single deposition chamber to deposit high-k dielectric films. Cheng and Fitzgerald[14] used metal organic chemical vapor deposition (MOCVD) and ALD to deposit ALD of high-k oxide on MOCVD deposited III-V compound semiconductor without vacuum break. Mantovan *et al.*[11] used their customized ALD/CVD system to deposit magnetic tunnel junctions. Our group built a multi-material hybrid ALD/CVD reactor back in 2009[18] and used this for CVD[19,20] and ALD[21–24] processes. All these papers used ALD/CVD hybrid apparatus for their respective application without discussing much about the system from equipment design point of view. This paper is intended to cover these aspects including control design.

In this paper, detailed descriptions are provided on the design and construction of precursor delivery system, oxidizer delivery system, UV-ozone generator, bubbler and control

a)Author to whom correspondence should be addressed. Electronic mail: takoudis@uic.edu

architecture of a portable ALD/CVD hybrid system. As a test of the system, ALD, CVD, and ALD/CVD hybrid films are deposited using this novel reactor system offering ALD precise thickness and composition control along with faster film growth capabilities of CVD. The resulting films are appropriately characterized to prove the effectiveness of the designed system. The reactor design is particularly suited for depositing all components of thin film intermediate temperature solid oxide fuel cell structures using ALD and CVD within single deposition system without vacuum break.

II. SYSTEM DESCRIPTION

The ALD/CVD hybrid system is a flow-type reactor. Three major sections of the system, the deposition chamber, precursor delivery system, and oxidizer delivery system are discussed in detail in Secs. II A–II E along with the precursor bubbler and ozone generator design.

A. Deposition chamber

The deposition chamber is a hot-wall, perpendicular-flow, aluminum chamber with optical diagnostic access. The chamber walls are heated by cartridge heaters and electrical heating tapes. The wafer stage is heated separately by two cartridge heaters located within the wafer stage, outside of the vacuum chamber. Detailed diagnostic flow analysis of the deposition chamber and computational flow analysis are reported elsewhere.[25] The precursors are kept in stainless steel (SS) bubblers and transported to deposition chamber through heated stainless steel tubes. The temperature is measured using glass braid insulated type-K thermocouple having accuracy of 2.2 °C. The system temperature is controlled by a single 6-zone proportional-integral-derivative controller (CN616, Omega Engineering, Inc.). The heating power controller consists of six solid state relays housed together in a grounded steel enclosure for portability. The reactor walls and delivery lines are heated ∼30 °C above precursor bubbler temperature to avoid precursor condensation. The wafer stage, delivery lines, and precursor bubblers can be heated up to 450 °C. High purity nitrogen (99.998% purity) is used to carry precursor vapor from the bubbler to the deposition chamber and to purge precursor/oxidizer out of the deposition chamber. A two stage, oil sealed rotary vane pump (Edwards Vacuum, Inc.) is used with zeolite fore line trap (13 × 10 Å; 1/8 in. pellets; Kurt J. Lesker Company). The zeolite trap prevents pump oil from back streaming into the deposition chamber as well as avoids precursors from getting into the pump. A manual ball valve is installed between the vacuum pump and the deposition chamber to isolate the deposition chamber during sample transfer and to regulate chamber pressure during deposition. A flexible, 1 m long, SS unbraided hose is used between pump and chamber to prevent pump vibration from reaching deposition chamber. The system has a base pressure of less than 40 mTorr and typically the ALD/CVD deposition is carried out at 500 mTorr. The deposition chamber is equipped with two pressure gauges covering the ranges of 1×10^{-3}-2 Torr range (Varian 801, Varian Inc.) and 1–760 Torr range (Series 902 Piezo transducer, MKS Instruments).

B. Precursor delivery line

Precursor delivery lines are carefully designed to accommodate ALD and CVD modes, minimize cost, improve compactness, and facilitate portability. The system has two delivery lines with a common by-pass line. Each line has two bellow-sealed pneumatic valves (Model: SS-BNVV51-C, Swagelok) and two manual plug valves (Model: SS-4P4T, Swagelok) arranged as shown in Fig. 1. Manual plug valves are used to protect air-sensitive precursor from coming in contact with air during precursor transfer. Oxidizer delivery is controlled by a 3-way bellow sealed switching valve (Model: SS-4BY-V35-1C, Swagelok). In ALD mode, valves V3 and V4 for line A or V5 and V6 for line B are opened momentarily, followed by precursor purging, oxidizer pulse, and oxidizer purge steps in a cyclic manner. V1 valve in bypass line is opened for precursor purging and oxidizer purging steps,

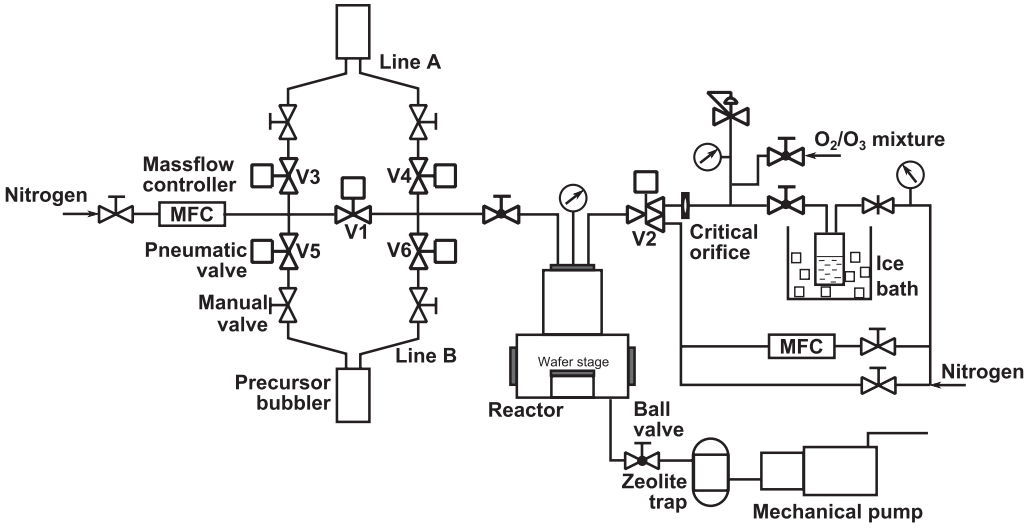

FIG. 1. Schematic diagram of the ALD/CVD hybrid reactor system.

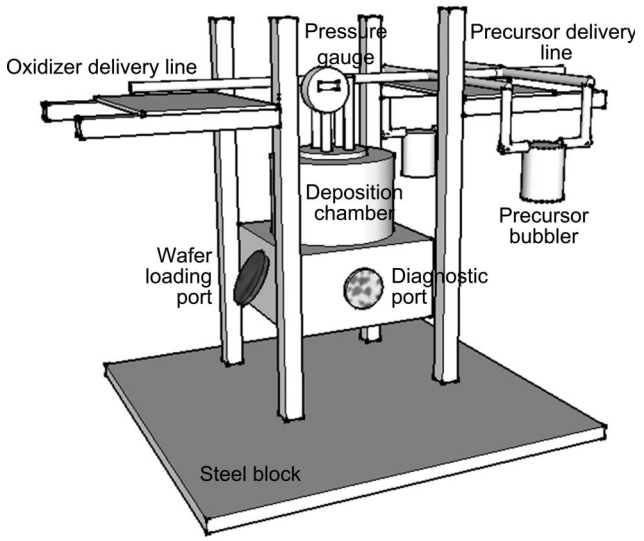

FIG. 2. Three-dimensional representation of the portable ALD/CVD system, showing the arrangement of precursor and oxidizer delivery lines. (Only major components are shown.)

whereas V2 is opened for the oxidizer pulse step. For CVD mode, V3 and V4 for line A or V5 and V6 for line B are opened along with oxidizer valve V2 for a specified time. This valve configuration allows for both ALD and CVD deposition modes within a single delivery system configuration. A custom-designed LabVIEW computer control program with I/O voltage interface electromechanically controls a series of miniature valves (Model: ET-3-24, Clippard Instrument Laboratory, Inc.) which, in turn, controls N_2 pressure to the pneumatic valves in the delivery lines. Thus, via computer command, the open/close sequencing of delivery valves is controlled for ALD or CVD operation which allows alternating between the two modes of operation thereby providing a more efficient means of synthesizing thick-thin (i.e., micro-nano) laminated film structures within a single hybrid processing chamber. All valves are bolted firmly on a 12 × 12 in. aluminum plate for rigidity; and mounted right on top of the deposition chamber for compactness. Deposition chamber, valve plates, and control system parts are so arranged to minimize footprint and improve rigidity as shown in Fig. 2.

C. Oxidizer delivery line

This system is capable of delivering pure oxygen, ozone/oxygen mixture, or water vapor to the deposition chamber. Water vapor is delivered as wet nitrogen created by passing N_2 over the head space of a water reservoir maintained at ice temperature. The dip tube within the water reservoir is deliberately cut to avoid nitrogen injection inside the water bath to reduce moisture content in the N_2 without requiring additional dilution or heating-up of downstream delivery lines to prevent water vapor condensation.[26] In this system, the open-ended dip tube was cut 1 in. above water level. This arrangement markedly reduced oxidizer purging time from 20 s to 10 s.[26] This oxidizer delivery line is connected with a proportional relief valve (Model: SS-RL3S4, Swagelok) and a pressure gauge to facilitate continuous stream of oxidizer at a set pressure (0.7 psi).

D. Bubbler design

Most vapor deposition systems use heated-open boat to deliver solid/low-vapor pressure liquid precursors and passivated stainless steel bubblers for moderate to high vapor pressure liquids. In this study, continuous flow CVD-type bubblers[27] are used to accommodate ALD and CVD operating modes. The precursor bubbler components are fabricated from 316L stainless steel, assembled using combination of tungsten-inert gas (TIG) and CO_2 laser welding techniques. Conflat® flanges with copper gasket are used to seal the bubbler reservoir to the top cap which has two Swagelok VCR® fittings (1/4 in. diameter, Model: 6LV-4-VCR-3-4TB7) TIG welded onto the cap for gas in and out ports. The fittings on the cap have manual plug valves at each end. Two kinds of bubbler are used, one with dip tube for most liquid precursors and another without dip tube (sublimator) for solid precursors or very high vapor pressure liquid precursors such as dimethyl zinc.[21] Wetted areas of the bubbler are electropolished internally and externally to minimize potential surface reactions and outgassing with the precursor. After electropolishing, the bubblers were sonicated in organic solvents (methanol and acetone) and baked at 200 °C overnight before loading the precursor into the bubbler.

E. Ozone generator

Ozone is commonly produced by two methods: corona discharge and UV lamp illumination. In corona discharge, an electric discharge split oxygen molecules within the discharge region and form ozone. Alternatively, an UV lamp that emits light in the far UV region (∼185 nm) can produce ozone by photolysis of oxygen molecules.[28] Although corona discharge produces a high concentration of ozone, a UV lamp produces more uniform concentration over long period of time which is preferred for this study. An important aspect of ozone generator design is the selection of sealing material, as even low level of ozone leak can also be harmful to respiratory tract and lungs.[29] Ozone being a strong oxidizer affects O-rings used for sealing. Viton®, Kalrez®, and Teflon® O-rings are reported to be more resistant to ozone attack.[30] Viton O-rings coated with a thin layer of Fomblin® high vacuum grease is used in this system. A 25 W UV germicidal lamp (Model: G24T5VH/U, Atlantic Ultraviolet Corporation) is used with suitable lamp holder and ballast. The lamp is housed within a 2.5 in. diameter aluminum cylinder with gas inlet and outlet ports. A four-pin, O-ring sealed power feedthrough is used to route the power cables of UV lamp through cylinder cap. Schematic diagram of our homemade UV-ozone generator is shown in Fig. 3. The generator is placed immediately upstream of the deposition chamber to reduce ozone decomposition in delivery line. With pure oxygen (99.999% purity) at 0.7 psi as inlet gas, our custom-built ozone generator produces about 1000 ppm of ozone, as measured with an ozone analyzer (Model 450, Advanced Pollution, Inc.).

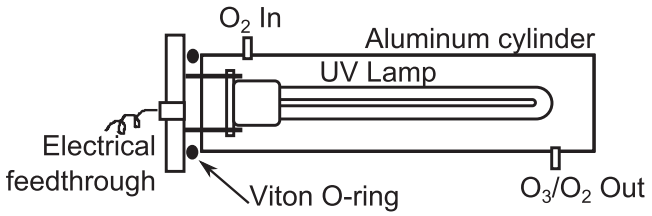

FIG. 3. Schematic diagram of homemade UV-ozone generator.

III. CONTROL SYSTEM IMPLEMENTATION

This section describes a simple way to write LabVIEW program to control ALD mode of operation in a single delivery line ALD/CVD hybrid system. LabVIEW (Version 11.0.1) block diagram of the program is shown in Fig. 4(a). This program takes number of ALD cycles (N_c), precursor pulse time, precursor purge time, oxidizer pulse, and oxidizer purge times as input, and controls the four pneumatic valves (V1-V4) located at precursor and oxidizer delivery lines. Valve position (True/False) for all four ALD sub-cycles are stored in "ALD Recipe" block in the form of two-dimensional (2D) array of Boolean constants. This 2D array is then fed to "Index Array-1" (IA-1) block. "Build Array" block build one-dimensional array of sub-cycle times and feed it to "IA-3." "IA" block returns the element or sub-array of n-dimension array at the supplied index number. This index number (0-3) is supplied by "Quotient and Remainder" block to IA-1 and IA-3, thus combining valve positions for a particular sub-cycle with its corresponding sub-cycle time. This valve position information is then send to Boolean indicators and "Data Acquisition" module (not shown) that communicates with valve-hardware; whereas, sub-cycle time is send to "Wait (ms)" block, that halts the LabVIEW program in the same valve positions for the specified sub-cycle time before switching to the next sub-cycle valve positions. The entire process repeats $4 \times N_c$ times in loop to cover all four ALD sub-cycles for N_c number of times. The ALD program described here is, however, a simplified version of the actual program that has few extra recipes (Fig. 4(b)) to include "wait time before deposition" and second precursor line.

IV. EXPERIMENTAL VERIFICATION

The ALD mode of reactor operation was demonstrated with ALD of TiO_2 using tetrakis(diethylamino)titanium (TDEAT) and water vapor. Deposition was carried out on highly doped p-type Si(100) substrates (resistivity 1–10 Ω cm) cut into 2 cm × 2 cm pieces. Radio Corporation of America standard cleaning (RCA SC-1) procedure was followed to clean the substrate prior to deposition. Deionized water (resistivity ≥ 17 MΩ cm) and nitrogen were used to clean the substrate after every RCA step. The substrates were loaded immediately after cleaning. Figure 5 shows the effect of precursor pulse duration on growth rate of TiO_2 films deposited at 200 °C with 1 s oxidizer pulse. Precursor and oxidizer purging times were optimally fixed at 15 and 10 s, respectively, after ensuring no change in the growth rate with longer purge times. The TDEAT bubbler temperature was kept constant at 65 °C. With increasing precursor pulse duration to 2 s, the film growth rate increases to 0.04 nm/cycle; no further increase in the growth rate was observed for longer precursor pulse durations beyond 2 s. This confirms the characteristic self-limiting growth behavior of ALD. Film growth rate was relatively insensitive to changes in oxidizer pulse time tested from 50 ms to 2 s (Fig. 6). The TiO_2 film growth rate dependence on reactor temperature is shown in Fig. 7; it is found to be independent of reactor temperature between 150 and 275 °C, indicating adsorption controlled growth regime. Figure 8 shows the film thickness measured after different number of ALD cycles. Good linearity demonstrates the thickness tunability with this reactor. The TiO_2 ALD growth rate is in good agreement with reported values in the literature.[31]

The composition of ALD TiO_2 films were probed with high resolution X-ray Photoelectron Spectroscopy (XPS)

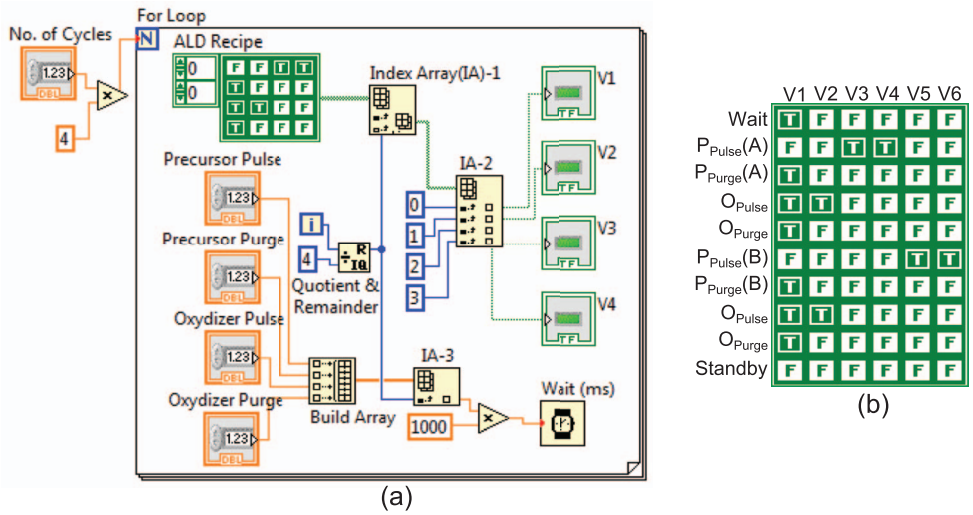

FIG. 4. (a) LabVIEW block diagram for ALD mode in a single delivery line ALD/CVD hybrid system. (b) ALD Recipe for ALD/CVD system with two delivery lines.

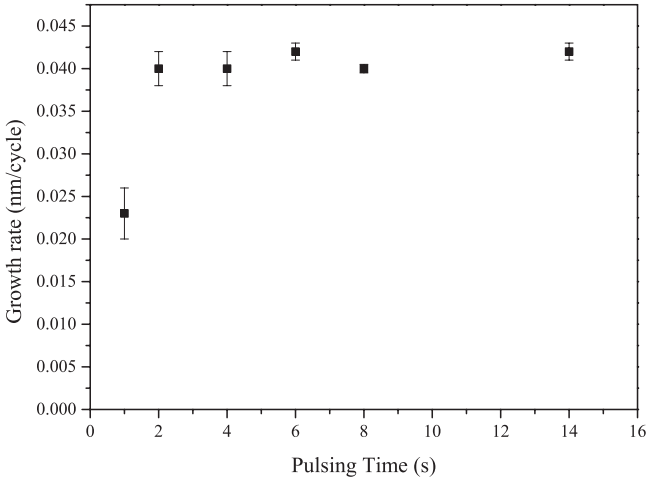

FIG. 5. Effect of precursor pulse time on TiO_2 ALD growth rate at 200 °C substrate temperature. The bubbler temperature was at 65 °C. The system pressure was 0.5 Torr. The vertical error bars indicate film uniformity across the sample.

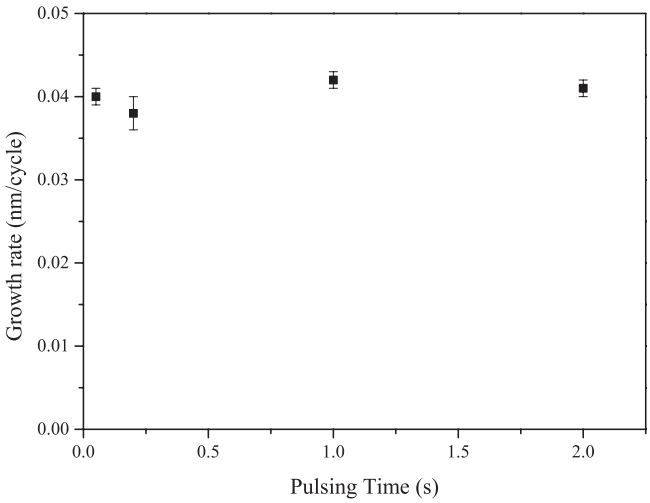

FIG. 6. Effect of oxidizer (water vapor) pulse time on TiO_2 ALD growth rate. All ALD conditions are the same as those in Fig. 5.

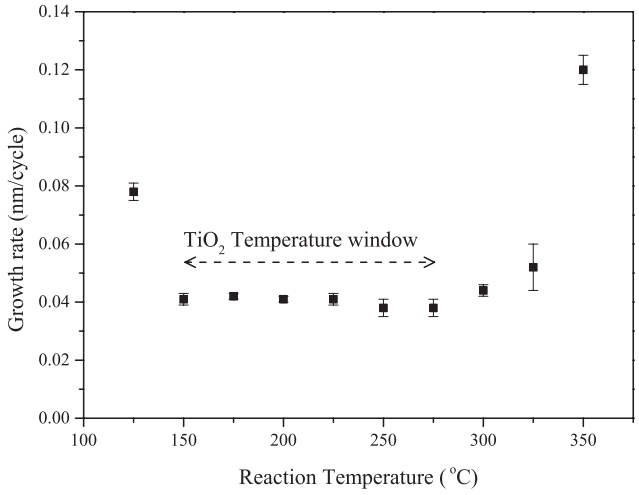

FIG. 7. TiO_2 ALD growth rate as a function of reactor temperature. Other conditions are the same as in Fig. 5.

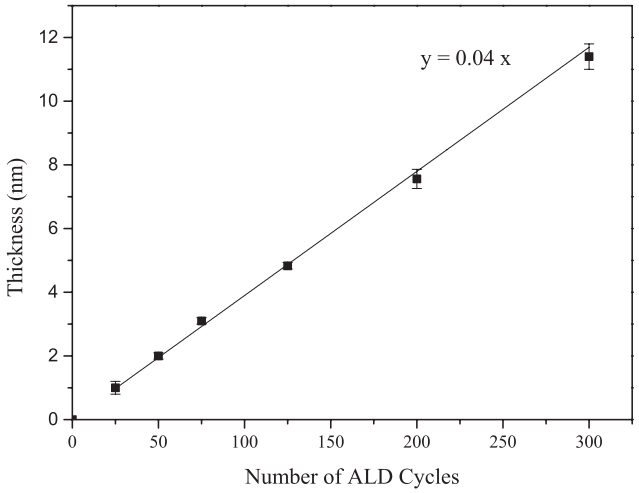

FIG. 8. TiO_2 ALD growth rate as a function of number of ALD cycles. The substrate was at 200 °C. The growth rate is constant at 0.04 nm/cycle.

(Kratos AXIS-165, Kratos Analytical Ltd.) equipped with a monochromatic Al Kα (1486.6 eV) X-ray source operating at 15 kV and 10 mA. Spectra were taken after sputtering the surface using ~100 nA Ar^+ beam for 20 min. Survey spectrum of 30 nm-thick film (Fig. 9) shows stoichiometric titanium oxide (Ti ~ 32 at. %; O ~ 66 at. %) with a trace amount of carbon (~2 at. %) and argon. Argon in the film most likely came from the Ar^+ beam sputtering, and it is omitted from elemental analysis.

The CVD mode of the reactor with similar delivery system has been used and reported earlier from our group.[19,20] A few CVD experiments were conducted with this reactor setup to probe the growth rate of SnO_x CVD using tin(II)acetylacetonate and ozone at 250 °C reactor temperature and 70 °C precursor bubbler temperature. The growth rate was found to be 0.7 nm/min, which is about half of the value reported with the same precursor but with a different reactor system having an order of magnitude higher gas flow rate than the system reported in this study.[32] The ALD/CVD hybrid mode was demonstrated using ALD of

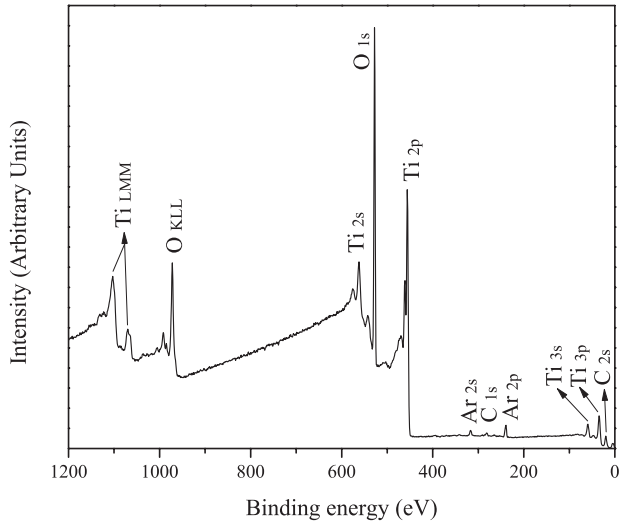

FIG. 9. XPS spectra for atomic layer deposited 30 nm-thick TiO_2 at 200 °C substrate temperature with TDEAT and water.

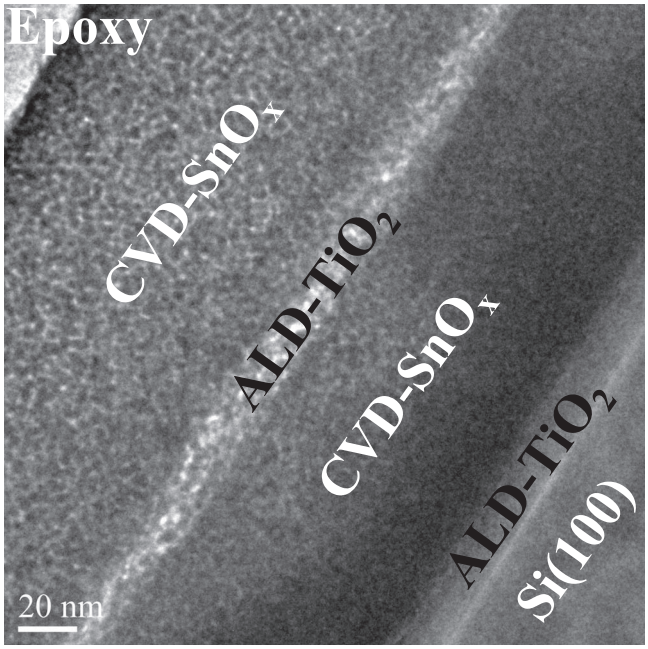

FIG. 10. Low magnification TEM image of as-deposited ALD-TiO_2/CVD-SnO_x hybrid film deposited at 250 °C substrate temperature.

TiO_2 and CVD of SnO_x at 250 °C. A prolonged 5 min N_2 purging was performed when changing from ALD mode to CVD mode or vice versa to avoid memory effects. This purging time is an order of magnitude higher than the purging time we use for ALD of TiO_2 and SnO_x in the same system. Thus, cross contamination between titanium and tin was therefore avoided/minimized. It is noted that this system has two purging lines, precursor purging line (also called bypass line) and oxidizer purging line (through 3-way switching valve) to ensure complete purging of remaining precursor and oxidizer out of deposition chamber. A low magnification transmission electron microscopy (TEM) image of as-deposited ALD-TiO_2/CVD-SnO_x is shown in Fig. 10. Distinct layers of ALD and CVD are observed. The thickness of layers are measured to be ~108 nm CVD-SnO_x : 10 nm ALD-TiO_2 : 82 nm CVD-SnO_x : 11 nm ALD-TiO_2 which corresponds to 150 min of CVD-SnO_x : 150 cycles of ALD-TiO_2 : 150 min of CVD-SnO_x : 150 cycles of ALD-TiO_2. The reduced thickness in the first CVD-SnO_x layer may be due to a possible phase change from prolonged exposure (~4 h more than the second CVD-SnO_x layer) to 250 °C during the deposition of the top layers. Fortunato *et al.*[33] reported phase change in tin oxide films when exposed to temperature as low as 200 °C for 1 h. Njoroge *et al.*[34] reported up to 9% increase in density when $Ge_2Sb_{2.04}Te_{4.74}$ films were annealed at 280 °C. All these, along with darker first CVD-SnO_x layer in the TEM image, suggest that phase change lead to tighter packing thereby lowered thickness of the first CVD-SnO_x layer. The 2 nm-thick bright layer between silicon substrate and ALD-TiO_2 layer is most likely a silicon oxide layer. These experiments and characterization results show successful deposition of ALD, CVD, and ALD/CVD hybrid layers using this reactor.

V. CONCLUSION

A portable ALD/CVD hybrid reactor setup is described and successfully tested with ALD of TiO_2, CVD of SnO_x, and ALD-TiO_2/CVD-SnO_x hybrid film depositions. TiO_2 ALD results demonstrate thickness tunability of the reactor for ALD deposition. The resultant film was analyzed with XPS and found to be stoichiometric TiO_2 with a trace amount of carbon. ALD rate and film purity are in good agreement with literature values. Deposition of ALD-TiO_2/CVD-SnO_x hybrid films proved the ability of the reactor to deposit thick-thin nano-laminate structures without vacuum break; TEM confirmed the distinct ALD and CVD layers. Changes in vapor delivery system and control architecture of conventional vapor deposition system paved the way to accommodate ALD and CVD modes of operation in a single portable deposition system.

ACKNOWLEDGMENTS

We gratefully acknowledge the National Institute of Standards and Technology (NIST) and Dr. James Maslar for providing the deposition chamber. TDEAT precursor was provided by Dr. Christian Dussarrat (Air Liquide Group). This project was supported by the National Science Foundation (NSF) (CBET 1067424).

[1]C. Wiemer, L. Lamagna, and M. Fanciulli, Semicond. Sci. Technol. **27**, 074013 (2012).
[2]Y.-N. Zhou, M.-Z. Xue, and Z.-W. Fu, J. Power Sources **234**, 310 (2013).
[3]J. J. Coleman, Proc. IEEE **85**, 1715 (1997).
[4]M. Ohring, *Materials Science of Thin Films*, 2nd ed. (Academic Press, San Diego, 2002), p. xiii.
[5]N. Selvakumar and H. C. Barshilia, Sol. Energy Mater. Sol. Cells **98**, 1 (2012).
[6]S. Haukka, E. L. Lakomaa, and T. Suntola, *Studies in Surface Science and Catalysis* (Elsevier, 1999), Vol. 120, Part A, p. 715.
[7]C. J. Hwang and S. W. Lee, U.S. patent 6530993 (11 March 2003).
[8]X. Zeng, A. V. Pogrebnyakov, A. Kotcharov, J. E. Jones, X. X. Xi, E. M. Lysczek, J. M. Redwing, S. Xu, Q. Li, J. Lettieri, D. G. Schlom, W. Tian, X. Pan, and Z.-K. Liu, Nature Mater. **1**, 35 (2002).
[9]K. G. Reid and A. Dip, U.S. patent 7816278 (19 October 2010).
[10]P. M. Martin, L. C. Olsen, J. W. Johnston, and D. M. Depoy, J. Vac. Sci. Technol. B **21**, 1384 (2003).
[11]R. Mantovan, S. Vangelista, B. Kutrzeba-Kotowska, S. Cocco, A. Lamperti, G. Tallarida, D. Mameli, and M. Fanciulli, Thin Solid Films **520**, 4820 (2012).
[12]S. Kala, B. R. Mehta, and F. E. Kruis, Rev. Sci. Instrum. **79**, 013902 (2008).
[13]S. M. Choi, K. C. Park, B. S. Suh, I. R. Kim, H. K. Kang, K. P. Suh, H. S. Park, J. S. Ha, and D. K. Joo, in *Proceedings of the 2004 Symposium on VLSI Technology Digest of Technical Papers, Hawaii, 15–17 June 2004* (IEEE, 2004), p. 64.
[14]C.-W. Cheng and E. A. Fitzgerald, Appl. Phys. Lett. **93**, 031902 (2008).
[15]T. Suntola and J. Hyvarinen, Annu. Rev. Mater. Sci. **15**, 177 (1985).
[16]L. Reijnen, B. Meester, F. de Lange, J. Schoonman, and A. Goossens, Chem. Mater. **17**, 2724 (2005).
[17]J. M. Gaskell, A. C. Jones, H. C. Aspinall, S. Przybylak, P. R. Chalker, K. Black, H. O. Davies, P. Taechakumput, S. Taylor, and G. W. Critchlow, J. Mater. Chem. **16**, 3854 (2006).
[18]C. G. Takoudis and M. K. Singh, "Multi-metal films, alternating film multilayers, formation methods and deposition system," U.S. provisional patent application 61251820 (15 October 2009).
[19]M. Singh, Y. Yang, C. G. Takoudis, A. Tatarenko, G. Srinivasan, P. Kharel, and G. Lawes, Electrochem. Solid-State Lett. **12**, H161 (2009).
[20]M. K. Singh, Y. Yang, C. G. Takoudis, A. Tatarenko, G. Srinivasan, P. Kharel, and G. Lawes, J. Nanosci. Nanotechnol. **10**, 6195 (2010).
[21]R. Xu, J. Huang, S. Ghosh, and C. G. Takoudis, ECS Trans. **41**, 229 (2011).

[22]R. Xu, S. K. Selvaraj, N. Azimi, and C. G. Takoudis, ECS Trans. **50**, 107 (2013).
[23]R. Xu and C. G. Takoudis, ECS J. Solid State Sci. Technol. **1**, N107 (2012).
[24]R. Xu, Q. Tao, Y. Yang, and C. G. Takoudis, Appl. Surf. Sci. **258**, 8514 (2012).
[25]W. A. Kimes, E. F. Moore, and J. E. Maslar, Rev. Sci. Instrum. **83**, 083106 (2012).
[26]P. Majumder, G. Jursich, A. Kueltzo, and C. Takoudis, J. Electrochem. Soc. **155**, G152 (2008).
[27]B. Sang and M. Konagai, Jpn. J. Appl. Phys. **35**, L602 (1996).
[28]J. R. Vig, J. Vac. Sci. Technol. A **3**, 1027 (1985).
[29]M. Lippmann, JAPCA **39**, 672 (1989).
[30]R. N. Peacock, J. Vac. Sci. Technol. **17**, 330 (1980).
[31]R. Katamreddy, V. Omarjee, B. Feist, and C. Dussarrat, ECS Trans. **16**, 113 (2008).
[32]T. Maruyama and Y. Ikuta, Sol. Energy Mater. Sol. Cells **28**, 209 (1992).
[33]E. Fortunato, R. Barros, P. Barquinha, V. Figueiredo, S. H. K. Park, C. S. Hwang, and R. Martins, Appl. Phys. Lett. **97**, 052105 (2010).
[34]W. K. Njoroge, H. W. Woltgens, and M. Wuttig, J. Vac. Sci. Technol. A **20**, 230 (2002).